Nat Hazards (2016) 81:1797–1810
DOI 10.1007/s11069-016-2156-9

ORIGINAL PAPER

Design rainfall in Qatar: sensitivity to climate change scenarios

Abdullah Al Mamoon[1,3] · Niels E. Joergensen[2] · Ataur Rahman[3] · Hassan Qasem[1]

Received: 17 February 2015 / Accepted: 2 January 2016 / Published online: 14 January 2016

Abstract Design rainfall is needed in the design of numerous engineering infrastructures such as urban drainage systems, bridges, railways, metro systems, highways and flood levees. Design rainfall is derived using regional frequency analysis approach based on observed rainfall data from a large number of stations within a homogeneous region. This paper provides an assessment of the possible impacts of climate change on design rainfalls in Qatar. The future climate conditions are established based on AR4 and A2 categories of emission scenarios (SRES) specified by the Intergovernmental Panel on Climate Change. Predicted 24-h annual maximum rainfall series for both the wet (NCAR-CCSM) and dry scenarios (CSIRO-MK3.5) for the Qatari grid points are extracted for three different periods, which are current (2000–2029), medium-term (2040–2069) and end-of-century climates (2080–2099). Using an *L*-moments-based index frequency approach, homogeneous regions are established and the best-fit distribution is then used to derive rainfall quantiles for average recurrence intervals (ARIs) of 2, 5, 10, 25, 50 and 100 years. The results show that there is no significant change in the design rainfalls in Qatar in the short term covering 2040–2069; however, a significant change is predicted at the end of century covering 2080–2099. Updated design rainfalls are estimated considering climate change scenarios for the period of 2080–2099 by averaging results from the wet and dry climate scenarios. The increase in 24-h annual maximum rainfall for the period 2080–2099 (compared with the current period 2000–2029) is found to be in the range of 68 and 76 % for 100-year ARI. For the typical design ARIs of 10–20 years, the increase in design rainfall is found to be in the range of 43 and 54 %. The method presented in this study can be applied to other arid regions, in particular to the Middle Eastern countries.

✉ Ataur Rahman
a.rahman@westernsydney.edu.au

[1] Ministry of Municipality and Urban Planning, Doha, Qatar

[2] COWI A/S, Doha, Qatar

[3] School of Computing, Engineering and Mathematics, Western Sydney University, Locked Bag 1797, Penrith, NSW 2751, Australia

Keywords Climate change · Design rainfalls · IDF · Qatar · Climate variability · *L*-moments

1 Introduction

Design rainfall is a basic input for hydrological models used in estimating design flows. These are required in the planning and design of numerous engineering infrastructure projects such as urban drainage systems, bridges, culverts, railways, highways and causeways. Design rainfall is commonly expressed as a three-way intensity–duration–frequency (IDF) relationship. In some countries, like Australia, design rainfall is known as intensity–frequency–duration (IFD) data.

Design rainfalls in a given region are generally derived based on historical rainfall data from a large set of gauged stations (Haddad et al. 2011; Haddad and Rahman 2014; Mamoon et al. 2014a). However, due to climate change, increase in the frequency and magnitude of extreme precipitation events has been reported at many locations around the world, irrespective of the mean annual precipitation trends (Yilmaz and Perera 2014). An increasing trend in extreme precipitation has been observed in some countries where the mean annual precipitation has shown decreasing trends (Meehl et al. 2007; Tryhorn and DeGaetano 2011). Observations of recent climate indicate that this increasing trend in precipitation data is likely to continue in the future due to global warming (Guo 2006).

Due to high temporal and spatial variability of precipitation, increase or decrease in rainfall will not be uniform in geographical space (Alexander et al. 2006). Numerous studies undertaken at different countries have demonstrated statistically significant trends in the historical rainfall data (e.g. Adamowski and Bougadis 2003; Leahy et al. 2004; Arnbjerg-Nielsen 2006; Landsea et al. 2010; Clarke et al. 2011; Chen et al. 2013; Laz et al. 2014). The trends in historical hydro-meteorological data challenge the 'stationarity' assumption in frequency analysis (Ishak et al. 2013; Ishak and Rahman 2014). This raises the question whether the IDF data derived at a given region based on historical rainfall data and stationarity assumption will be valid for the design of engineering infrastructure projects to cater for future needs.

A number of studies have demonstrated the need to revise the existing IDF data based on the identified trends in historical precipitation data. For example, Guo (2006) assessed the impacts of the identified increase in heavy rainfall events on the design and operation of urban drainage systems in Chicago, USA, using an IDF relationship. Wang et al. (2013) assessed climate change impact on IDF curves at the Apalachicola River Basin, Florida, using a group of regional climate models (RCMs) under emission scenario A2. The extreme rainfall intensity and frequency were projected to increase by most of the selected models. Madsen et al. (2009) examined trends in extreme rainfalls in Denmark and found a general increase in extreme rainfall characteristics due to climate change. Lelieveld et al. (2012) suggested that the Eastern Mediterranean and the Middle East (EMME) are likely to be greatly affected by climate change, associated with increases in the annual precipitation in the Arabian Gulf area. Analysis and characterization of trends in rainfall data in the Arabian Peninsula and Gulf regions are particularly challenging, mainly due to the limited availability and poor quality of rainfall data (Nasrallah and Balling 1993; Zhang et al. 2005; Kwarteng et al. 2009). A review of the studies that examined trends in rainfall data in these regions demonstrated a high degree of variation in climatic conditions associated

with mixed trends (Elagib and Addin 1997; Zhang et al. 2005; AlSarmi and Washington 2011; Almazroui et al. 2012).

The IDF relationship for Qatar was initially derived by Bazaraa and Ahmed (1991), which has recently been updated (Mamoon et al. 2014b). This new IDF relationship for Qatar has been developed using a *L*-moments-based regional frequency analysis approach (Hosking and Wallis 1993), which did not consider the impacts of climate change. The objective of this study is to assess how the IDF relationship for Qatar is likely to be affected by climate change.

2 Study area and data selection

This study uses data from the state of Qatar. Qatar lies within an arid subtropical area where rainfalls are mainly concentrated in the period from October to May. The average annual rainfall measured at Doha International Airport in Qatar from 1962 to 2012 is 78.1 mm. The precipitation varies over Qatar with the highest rainfall in the northern part and the lowest in the southern part. The annual maximum series (AMS) of 24-h rainfall data from 32 stations located in Qatar and nearby Gulf countries have been used to develop the current IDF curves for Qatar (Mamoon et al. 2014b). Further information on the database used to derive the IDF curves in Qatar can be seen in Mamoon et al. (2013).

3 Methods

3.1 Development of current IDF curves in Qatar

An *L*-moments-based index regional frequency analysis method, introduced by Hosking and Wallis (1993), was used to derive the current IDF curves for Qatar. The *L*-moments-based index frequency approach can be expressed by the following equation:

$$I_i(T) = \bar{I}_i \times X_T \tag{1}$$

where $I_i(T)$ is T-year rainfall quantile (for a given duration) at site i and $\bar{I}_i$ is scaling factor at site i, e.g. mean annual maximum rainfall (for the given duration). For gauged site, $\bar{I}_i$ is taken as the at-site mean value, and for an ungauged site, it is estimated from regional prediction equation. Here, X_T is regional growth factor, which is the same for all the sites (gauged or ungauged) within a homogeneous region.

The *L*-moments-based frequency analysis approach (Hosking and Wallis 1993) has been widely adopted in hydrology (Bates et al. 1998; Rahman et al. 1999; Ishak et al. 2011). The implementation of the *L*-moments-based index frequency approach involves the following five steps:

1. *Data screening* This is done using a discordant measure (D_i), where a site with $D_i \geq 3$ is regarded as discordant. Any site flagged out as discordant needs to be examined for possible data error and other physical reason for possible removal of the site from the proposed homogeneous region.
2. *Testing for regional homogeneity* The heterogeneity measure (H_i) is calculated based on a Monte Carlo simulation. For $H_1 < 1$, the proposed region is regarded as 'acceptably homogeneous', for $1 \leq H_1 < 2$, the region is regarded as 'possibly heterogeneous', and for $H_1 \geq 2$, the region is regarded as 'definitely heterogeneous'.

3. *Identification of the best-fit distribution* This is based on a Z statistic; for a number of candidate distributions, the distribution(s) exhibiting $\left|Z^{DIST}\right| \leq 1.64$ is considered to be acceptable.
4. *Computation of regional growth curve* This involves estimation of weighted average growth curve from the at-site growth curves, which is applicable to any site within the homogeneous region.
5. *Quantile estimation* For gauged site, rainfall quantiles were estimated using Eq. (1). For ungauged sites, a regional prediction equation to estimate mean annual maximum rainfall was developed based on the data of the gauged sites. To assess the accuracy of the developed regional frequency analysis method, a leave-one-out (LOO) validation method was adopted (Haddad et al. 2013). The LOO, in essence, offers an independent testing of the developed regional frequency model by assuming each of the sites being ungauged in each of the iterations.

3.2 Development of future IDF curves

The Intergovernmental Panel on Climate Change (IPCC) (Meehl et al. 2007) developed four main emission scenarios and more sub-scenarios as noted in the IPCC Special Report on Emissions Scenarios 2000 (SRES) (Fig. 1) (IPCC 2000). There are four different sets of scenarios known as families, which are A1, A2, B1 and B2. A total of 40 SRES scenarios have been developed, which are equally valid in an analysis.

In this study, the A2 family is considered; according to IPCC (2000), the A2 world is characterized by (1) lower international cooperation than the A1 or B1 worlds; (2) lower mobility in people, ideas and capital resulting in slower diffusivity in technology; and (3) declined fertility rate. In A2, economic development is assumed to be regionally oriented

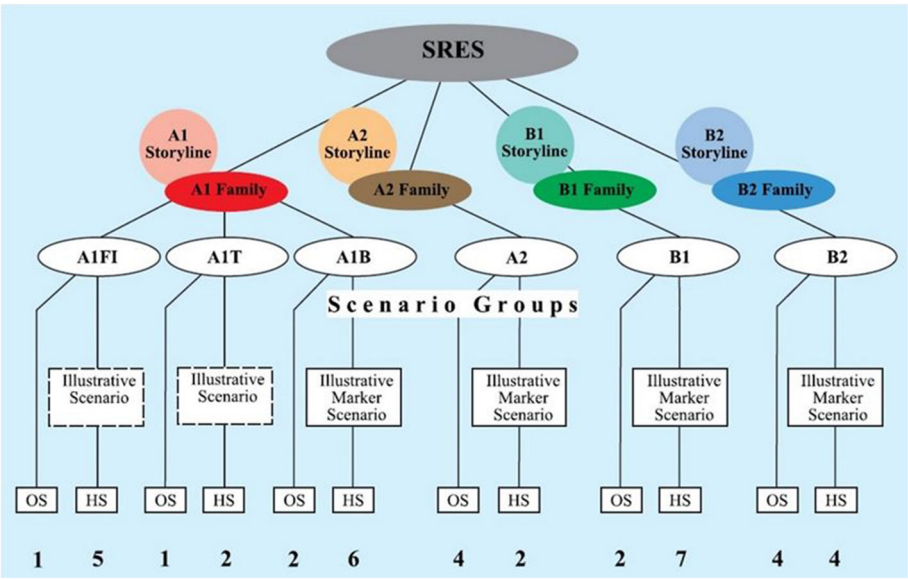

Fig. 1 SRES scenarios (Meehl et al. 2007)

and per capita economic growth and technological changes are taken to be more fragmented and slower as compared to other storylines.

This paper covers two different 50-year periods up to year 2100. In the first period, the climate changes are limited and of the same magnitude for the individual SRES scenarios, while change in temperature seems to be accelerating in the period from 2040 to 2100.

IPCC used results from 22 general circulation models (GCM) in the fourth assessment report (AR4). The largest grid size used in climate models is around 200 km × 200 km. There are differences between the predictions from the GCM models due to different focus and uncertainties related to climate modelling. Therefore, it is recommended not to use only one GCM, but to use a weighted average or more than one model to observe the span and variability. Two climate scenarios for Qatar were used in this study. For these scenarios, data analysis was carried out with a focus on precipitation for present and future situations. Four time periods were adopted for the evaluation of extreme rainfall: a measured historical period from 1962 to 2012, a current modelled period from 2000 to 2029, a future modelled period from 2040 to 2069 and another future modelled period from 2080 to 2099. To maintain temporal consistency between the data sets, all the data used in this analysis are annual maximum daily rainfall data for a 24-h duration. It should be noted that for annual average rainfall, however, the current period is considered to be 1961–1990, allowing comparison with actual measurements.

4 Results

4.1 Current IDF curves

The proposed region consisting of 32 stations from Qatar and nearby Gulf countries was found to be 'acceptably homogeneous' as the H values were found to be smaller than 1. The 32 stations represented 1185 station-year of observations with the oldest observation from year 1934 in Sharjah, United Arab Emirates. The best-fit distribution for 24-h duration AMS was found to be Pearson type 3, which was adopted as the regional probability distribution to develop the regional growth curve. For ungauged site application, a prediction equation was developed where mean annual maximum rainfall was expressed as a function of climatic and physical characteristics. From a LOO validation, it was found that the developed prediction equation could estimate mean annual maximum rainfall intensity with a median relative error value of 5.5 %. Finally, an approximate method was adopted to derive the design rainfalls for other durations as detailed in Mamoon et al. (2014b).

Empirical relationships for the rainfall depth ratios, expressed as P_d/P_{24h}, where P_d is the rainfall depth for the duration d and P_{24h} the daily rainfall depth, have been provided by World Meteorological Organization (WMO) and Indian Meteorological Organization (IMD) for $d < 24$ h. These rainfall depth ratios were compared with the rainfall depth ratios derived from the observed data at the Seeb (Oman) and Doha Airports (Qatar). The 10-min value for Doha International Airport was estimated based on the 10-min rainfall depth ratio given for Seeb Airport and the ratio between the 1-h rainfall depth ratio of Doha Airport and Seeb Airport. To correct for the restricted duration (for 24-h duration), as per Dwyer and Reed (1995), a correction factor α_D of 1.16 was adopted to convert from 24-h, restricted frame to 24-h, unrestricted frame, rainfall quantile. The unrestricted rainfall intensity can be expressed as $I_{i,u}$ given as:

$$I_{i,u}(T) = \alpha_D \times \bar{I}_i \times X_T \quad (2)$$

To derive the complete set of IDF curves, an approximate technique based on Kimijima method was adopted. An example set of IDF curves for Qatar developed by the above method is shown in Fig. 2. The derived IDF curves include the correction factor α_D of 1.16.

4.2 IDF curves for future climate

The CGM model results for the period (2000–2029) were used as baseline, indicating current climate. The rate of change from this modelled baseline until the modelled period (2040–2069), $C_{2040-2069}$, and the rate of change from the baseline to the modelled period (2080–2099), $C_{2080-2099}$, were applied on the regional growth curves to predict future growth curves.

$$I_{i,u,a}(T) = \alpha_D(1 + C_{a,T}) \times \bar{I}_i \times X_T \quad (3)$$

where a indicates a future period and $C_{a,T}$ is the rate of change in the average 24-h annual maximum rainfall from the current baseline period (2000–2029) to the climate change scenario for the period a, for a given T-year event. The rate of change is indicated in Fig. 7 for the period 2080–2099.

Referring to Eq. (3), the future site-specific growth curves for unrestricted rainfall intensity for Doha International Airport is based on the correction factor between restricted and unrestricted frame, rate of change from current to future scenario, the regional growth curve and the average 24-h annual maximum rainfall at the site. The 24-h annual maximum rainfall for Doha is determined from local measurements from 1962 to 2012. The two chosen combinations of GCM models and SRES scenarios used in this study are presented in Table 1.

The two scenarios provide quite a different average daily precipitation value. NCAR-CCSM/SRES A2 model indicates an average (1961–1990) daily average precipitation of approximately 0.9 mm/day, while the dry scenario CSIRO-MK3.5/SRES A2 predicts

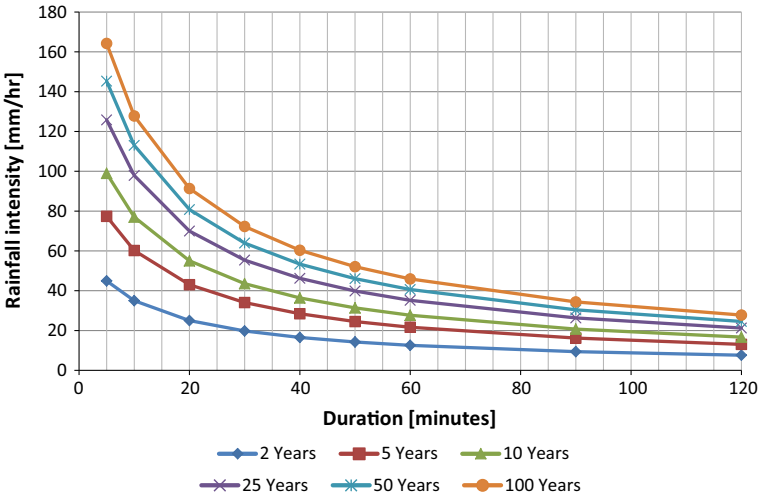

Fig. 2 IDF curves at Doha International Airport

Table 1 Annual average daily rainfall (mm/day)

	'Global Wet', NCAR-CCSM, SRES A2				'Global Dry', CSIRO-MK3, SRES A2			
	Latitude	Longitude			Latitude	Longitude		
		49.22	50.63	52.03		48.75	50.63	52.5
1961–1990								
mm/day	27.31	0.39	0.61	0.64	27.04	0.31	0.18	0.19
Yearly	25.91	0.55	0.72	0.78	25.17	0.22	0.17	0.16
Average	24.51	0.71	1.04	1.06	23.31	0.11	0.14	0.14
	23.11	0.59	0.93	1.29				
2040–2069								
Change in	27.31	0.319	0.308	0.305	27.04	−0.003	0.008	−0.025
mm/day	25.91	0.436	0.433	0.385	25.17	0.016	0.022	−0.004
Yearly	24 51	0.424	0.584	0.584	23.31	0.006	0.02	−0.001
Average	23.11	0.352	0.511	0.644				
2080–2099								
Change in	27.31	0.429	0.426	0.391	27.04	0.012	0.026	0.007
mm/day	25.91	0.632	0.707	0.513	25.17	0.016	0.014	−0.007
Yearly	24.51	0.622	0.914	1.011	23.31	−0.022	−0.006	−0.001
Average	23.11	0.545	0.79	1.147				

Table 2 Increase in annual average daily precipitation as a percentage of the present modelled precipitation in 1961–1990

	'Global Wet', NCAR-CCSM, SRES A2				'Global Dry', CSIRO-MK3, SRES A2			
	Latitude	Longitude			Latitude	Longitude		
		49.22	50.63	52 03		48.75	50.63	52.5
1961–1990								
mm/day	27.31	0.39	0.61	0.64	27.04	0.31	0.18	0.19
Yearly	25.91	0.55	0.72	0.78	25.17	0.22l	0.17	0.16
Average	24.51	0.71	1.04	1.06	23.31	0.11	0.14	0.14
	23.11	0.59	0.93	1.29				
2040–2069								
% Increase	27.31	82 %	50 %	48 %	27.04	−1 %	4 %	−13 %
mm/day	25.91	79 %	60 %	49 %	25.17	7 %	13 %	−3 %
Yearly	24.51	60 %	56 %	55 %	23.31	5 %	14 %	−1 %
Average	23.11	60 %	55 %	50 %				
2080–2099								
% Increase	27.31	110 %	70 %	61 %	27.04	4 %	14 %	4 %
mm/day	25.91	115 %	98 %	66 %	25.17	7 %	8 %	−4 %
Yearly	24.51	88 %	88 %	95 %	23.31	−20 %	−4 %	−1 %
Average	23.11	92 %	85 %	89 %				

0.17 mm/day. The average daily precipitation during the period 1962–2012 at Doha International Airport is 78.1 mm/year or 0.21 mm/day on average. There is a significant increase in average precipitation over the whole period in scenario NCAR-CCSM/SRES A2. There is no pronounced increase in average precipitation scenario for CSIRO-MK3.5/SRES A2; however, there is a limited increase in the first period followed by a decrease, while the total increase in 2080–2099 is less than the increase up to 2040–2069.

Table 2 shows the increase as a percentage of the modelled average annual precipitation compared with the 1961–1990 value. It can be seen that the increase in average precipitation is almost 100 % up to year 2100 in the wet scenario NCAR-CCSM/SRES A2, while the resulting increase in the dry scenario CSIRO-MK3.5/SRES A2 is limited to 10 %. The predicted average daily precipitation for 2080–2099 is 1.4–2 mm in the wet scenario and approximately 0.2 mm in the dry scenario. The maximum 24-h precipitation estimates from each GCM is used to develop estimates of the 2-, 10-, 20-, 50- and 100-year ARI 24-h rainfall depth using the Pearson type 3 distribution (i.e. the same distribution is used for the current and future conditions).

The IDF curves for the extreme storms with different ARIs were established directly from the given predicted future climate data for the two climate scenarios for the year 2050 and year 2100, respectively. The 24-h annual maximum rainfalls were found for three modelled periods 2000–2029, 2040–2069 and 2080–2099. The ARIs for 24-h maximum rainfall for the different periods were based on the assumption that the 24-h maximum (sliding/unrestricted frame) was 16 % higher than the 24-h (fixed/restricted frame) maximum (Dwyer and Reed 1995). Hence, the correction factor was taken as $\alpha_D = 1.16$, and the maximum rainfall in the future was assumed to have a Pearson type 3 distribution. Furthermore, it was assumed that the local areal reduction factor (ARF) would follow a logarithmic function, as suggested by Steward (1989). The cell sizes in the GCM models were approximately 43,000 km^2 and 24,000 km^2; hence, the ARF was extrapolated. The

Fig. 3 Grid cells used from the two GCM models (CSIRO-MK3.5 in *top* and NCAR in *bottom*)

average maximum precipitation in the cell must be compensated by the ARF depending on the cell size, so the expected maximum precipitation could be derived at a spot point (as a rain gauge) and compared to the derived IDF curves. For NCAR and CSIRO mesh sizes, the ARF was expressed as a logarithmic function of the return period.

The location of the GCM cells for NCAR and CSIRO-MK3.5 models is depicted in Fig. 3. For NCAR, the geographical footprint of Qatar covers four cells. It was assumed that the four cells form a homogeneous region and the adopted regional frequency analysis was applicable. For CSIRO-MK3.5, the mesh size is larger and the geographical footprint of Qatar is covered by a single cell. Here, the preferred statistical distribution and its parameters can be determined directly without applying regional frequency analysis. It was assumed that the NCAR, CSIRO and the preferred regional frequency analysis regions formed based on measured data were comparable despite the geographical differences. The H and Z statistics were computed (Table 3). It should be noted that NCAR region was found to be heterogeneous for the model prediction year 2040 to 2069 (H_1 greater than 2). Furthermore, the rainfall data for the CSIRO-MK3.5 model, year 2040–2069, followed a generalized Pareto distribution. However, it was assumed that a Pearson type 3 distribution could be applied despite the Z statistic being 3.1.

The growth curves for the existing condition (2000–2029) modelled by the NCAR and CSIRO-MK3.5 are shown in Fig. 4. It can be seen that the modelled growth curve for the CSIRO-MK3.5 model (green curve) yields results closer to the measured growth curve (blue curve). It should be noted that the dry model (CSIRO-MK3.5) has a restricted average annual maximum 24-h rainfall of 21.7 mm, compared to the wet model (NCAR) value of 24.05 mm, which is very close to the measured average value of 24.84 mm. The dry model (CSIRO-MK3.5) predicts a higher likelihood for extreme events. It is expected that most of the GCM models will deliver results within the range predicted by the two models used here, represented by the very wet and very dry conditions. It appears that there is a significant shift towards more extreme weather patterns at the end of the current century. In the intermediate period between the current situation and the time period 2040–2069, the predicted rate of change is modest (Fig. 5). Both the models indicate that

Table 3 Summary of H and Z statistics for the observed data, the NCAR model and the CSIRO-MK3.5 model outputs

Model	Observations selected region	NCAR			CSIRO-MK3.5		
Period	1962–2012	2000–2029	2040–69	2070–99	2000–2029	2040–69	2070–99
Average Daily Ann. Max (mm)	24.84	24.05	25.25	28.53	21.70	17.54	27.98
H-Stats [H(1)]	0.952	0.566	6.78	−1.149	NA	NA	NA
H-Stats (H(2))	0.567	−0.568	0.817	−1.815	NA	NA	NA
H-Stats [H(3)]	0.462	−0.646	−0.827	−1.858	NA	NA	NA
Z-Stats	−0.61	0.55	1.05	−1.29	0.8	3.1	0.58
Pearson type 3—parameters							
Average (μ)	1.0000	1.0000	1.0000	1.0000	1.0000	1.0000	1.0000
SD (σ)	0.667	0.352	0.365	0.583	0.567	0.574	0.823
Skewness (γ)	1.299	1.267	1.084	1.716	0.961	0.589	1.408

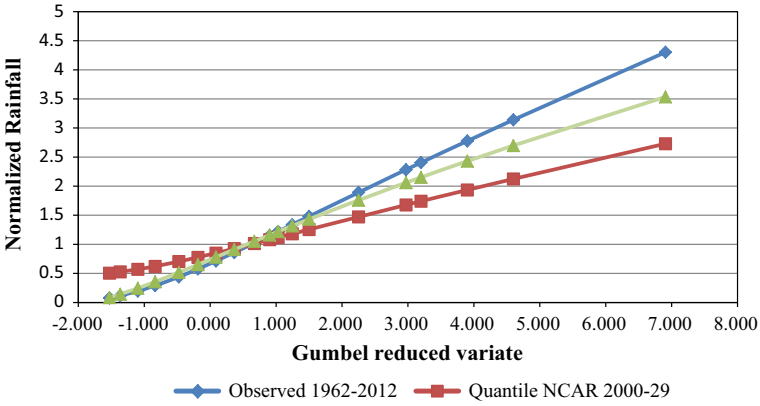

Fig. 4 Comparison of growth curves between climate models NCAR and CSIRO-MK3.5 for periods 1962–2012 (observed data) and 2000–2029 (future period)

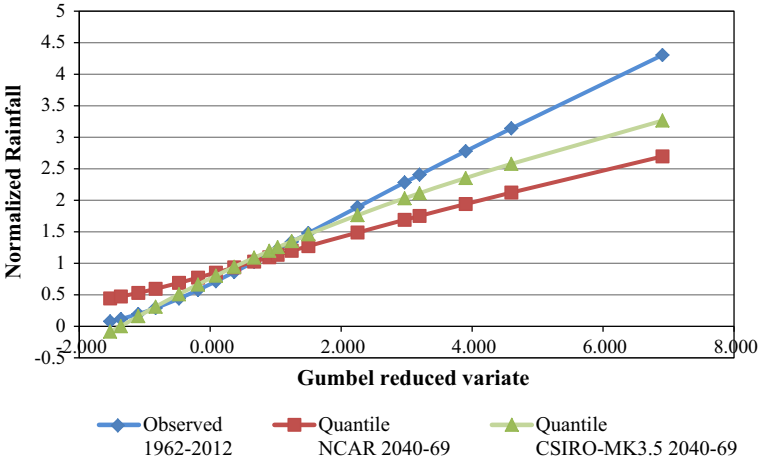

Fig. 5 Comparison of growth curves between climate models NCAR and CSIRO-MK3.5 for periods 1962–2012 (observed data) and 2040–2069 (future period)

there will be no increase in the extreme rainfalls generally, but there will be a slight decrease in the annual maximum 24-h rainfall during the next 40 years.

The significant changes in rainfalls appear to take place in the second time period 2080–2099 (Fig. 6) by the dry model (CSIRO-MK3.5). For a 100-year rainfall event (equivalent to Gumbel reduced variate of 4.6), the dry model (CSIRO-MK3.5) predicts a rainfall quantile of 3.7 mm/h, which is 2.88 mm/h for the wet model (NCAR). This is equivalent to 88.8 mm (for dry model) and 69.12 mm (for wet model) for a 24-h duration, i.e. a difference of 28 %.

The rate of change of 24-h annual maximum rainfall between the modelled current period (2000–2029) and future period (2080–2099) for the wet and dry models is shown in Fig. 7. As can be seen, both the dry and wet models predict nearly the same relative

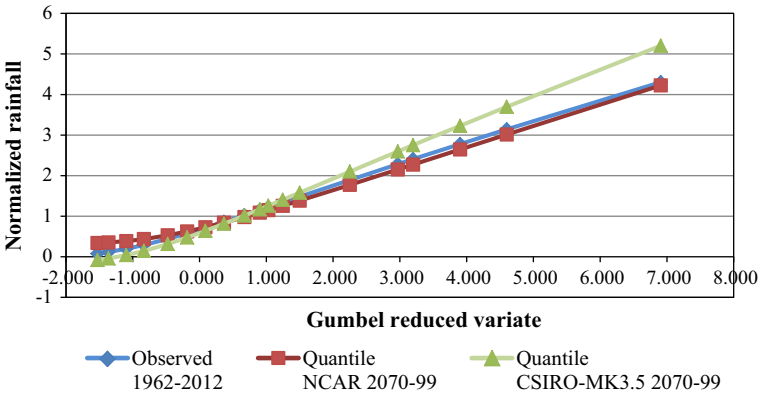

Fig. 6 Comparison of growth curves between climate models (NCAR/CSIRO-MK3.5) 2080–2099 and observed data (1962–2012)

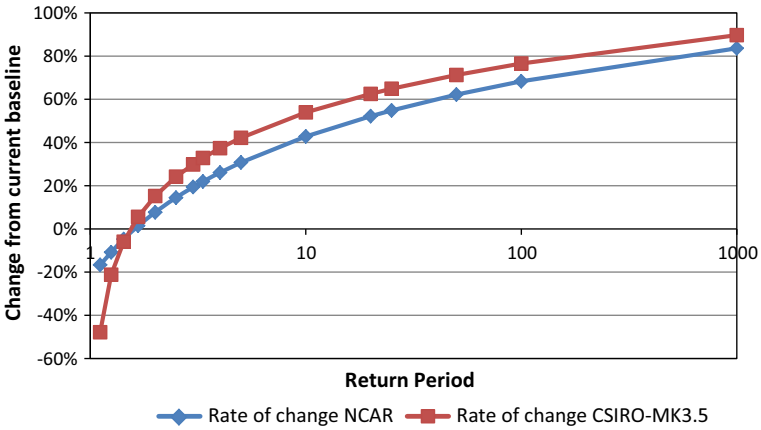

Fig. 7 Rate of change in average 24-h annual maximum rainfall as a function of the return period (years) between the current period (2000–2029) to future period (2080–2099) as per NCAR and CSIRO-MK3.5 models

change, resulting in an increase between 68 and 76 % for a 100-year rainfall event. For the typical design return periods of 10–20 years, the increases are between 43 and 54 %.

The resulting IDF curves for the future scenario at Doha International Airport Station, Qatar, are shown in Fig. 8. Here, the future IDF curves are developed using the rate of change (Fig. 7) to the existing IDF curves. The wet and dry scenarios are represented by the NCAR 2080–2099 and CSIRO-MK3.5 2080–2099 models, respectively, as mentioned before.

The baseline depth–duration–frequency curves (DDF), based on existing observed condition, and the future wet and dry scenarios for the annual maximum 24-h rainfall are shown in Fig. 9 for the purpose of comparison. As can be seen, the application of the rate of change on the existing condition will influence the design rainfall significantly, while applying the models directly will increase the design rainfall modestly.

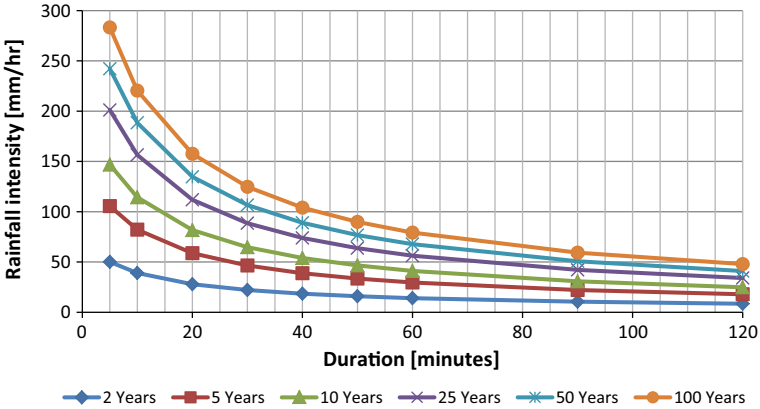

Fig. 8 IDF curve for Doha under future climate conditions (year 2080–2099)

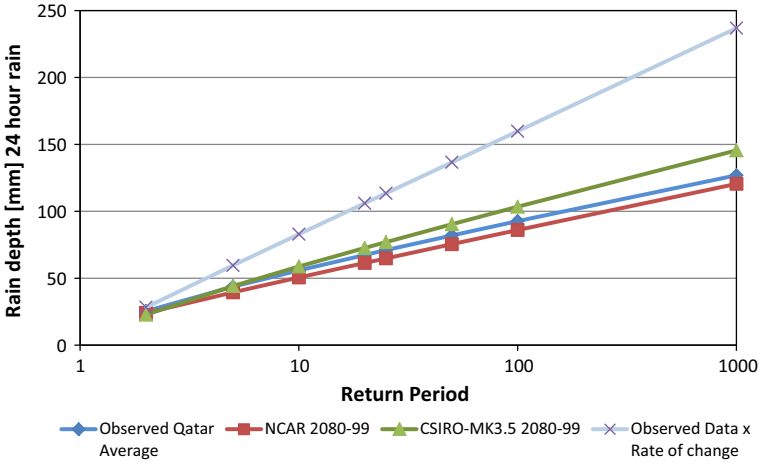

Fig. 9 DDF curves for observed data, NCAR (2080–2099) and CSIRO-MK3.5 (2080–2099)

The IDF curves shown in Fig. 8 were developed based on the precautionary principle of taking the 'worst-case' scenario; thus, the rate of change was applied on the observed data for Qatar. Furthermore, it was assumed that the same short duration rainfall ratios of 24-h rainfall could be applied for the current scenario. Precaution should be exercised in applying these results in practice for the following reasons:

- Actual ARF curves for Qatar, based on Qatari observations, have not been developed yet. The ARF curves applied here are derived from the UK data having a different climate.
- It is assumed that the future ARFs remain unchanged compared to the existing condition. This assumption may not hold as greater temporal and spatial variations may be expected in the future.
- The rate of change has been based on the extreme climate change scenarios (wet and dry conditions).

- The grid sizes in the climate change models are quite large, and the model will provide coarse rainfall data, not easily comparable with point rainfall data or rainfall on smaller catchments.

5 Conclusion

This paper provides an assessment of possible impacts of climate change on design rainfalls in Qatar. The future climate conditions are established based on the AR4 and A2 emission scenarios (SRES) specified by IPCC. For the derivation of design rainfalls, annual maximum series of predicted 24-h rainfall data for both the wet (NCAR-CCSM) and dry (CSIRO-MK3.5) scenarios for the Qatari grid points is extracted for three different periods: current (2000–2029), medium-term (2040–2069) and end-of-century climates (2080–2099). Using an *L*-moments-based index frequency approach, homogeneous regions for the Qatari grid points are established and the best-fit distribution is then used to derive rainfall quantiles for six different average recurrence intervals (ARIs). The results show that there is no significant change in the design rainfalls in Qatar in the short term (2040–2069); however, a significant change is predicted at the end of the century (2080–2099). New design rainfalls are developed considering climate change scenarios for the period 2080–2099 by averaging results from the wet and dry climate scenarios. The increase in 24-h design rainfall for the period 2080–2099 (compared with the current period 2000–2029) is found to be in the range of 68 and 76 % for a 100-year ARI. For the typical design ARIs of 10–20 years, the increase in 24-h design rainfall is found to be in the range of 43 and 54 %. The methodology developed in this study can be applied to neighbouring countries in the Gulf region for assessing design rainfalls by incorporating the impacts of climate change.

Acknowledgments The authors acknowledge the Meteorology Department of Qatar Civil Aviation Authority, Bahrain Civil Aviation Authority, Sharjah Airport and Qatar Ministry of Environment for providing the data used in this study.

References

Adamowski K, Bougadis J (2003) Detection of trends in annual extreme rainfall. Hydrol Process 17:3547–3560

Alexander LV, Zhang X, Peterson TC, Caesar J, Gleason B et al (2006) Global observed changes in daily climate extremes of temperature and precipitation. J Geophys Res Atmos 111:D05109. doi:10.1029/2005JD006290

Almazroui M, Islam MN, Jones PD, Athar H, Rahman MA (2012) Recent climate change in the Arabian Peninsula: seasonal rainfall and temperature climatology of Saudi Arabia for 1979–2009. Atmos Res 111:29–45

AlSarmi S, Washington R (2011) Recent observed climate change over the Arabian Peninsula. J Geophys Res 116:D11109

Arnbjerg-Nielsen K (2006) Significant climate change of extreme rainfall in Denmark. Water Sci Technol 54(6–7):1–8

Bates BC, Rahman A, Mein RG, Weinmann PE (1998) Climatic and physical factors that influence the homogeneity of regional floods in south-eastern Australia. Water Resour Res 34(12):3369–3381

Bazaraa AS, Ahmed S (1991) Rainfall Characterization in an arid area. Engineering Journal of Qatar University, Department of Civil Engineering, Doha, Qatar

Chen YR, Yu B, Jenkins G (2013) Secular variation in rainfall and intensity-frequency-duration curves in Eastern Australia. J Water Clim Change 4(3):244–251

Clarke C, Hulley M, Marsalek J, Watt E (2011) Stationarity of AMAX series of short-duration rainfall for long-term Canadian stations: detection of jumps and trends. Can J Civ Eng 38:1175–1184

Dwyer IJ, Reed DW (1995) Allowance for discretization in hydrological and environmental risk estimation. Institute for Hydrology, Wallingford
Elagib NA, Addin AAS (1997) Climate variability and aridity in Bahrain. J Arid Environ 36:405–419
Guo Y (2006) Updating rainfall IDF relationships to maintain urban drainage design standards. J Hydrol Eng 11:506–509
Haddad K, Rahman A (2014) Derivation of short duration design rainfalls using daily rainfall statistics. Nat Hazards 74:1391–1401
Haddad K, Rahman A, Green J (2011) Design rainfall estimation in Australia: a case study using L moments and generalized least squares regression. Stoch Environ Res Risk Assess 25(6):815–825
Haddad K, Rahman A, Zaman M, Shrestha S (2013) Applicability of Monte Carlo cross validation technique for model development and validation using generalized least squares regression. J Hydrol 482:119–128
Hosking JRM, Wallis JR (1993) Some statistics useful in regional frequency analysis. Water Resour Res 29(2):271–281
IPCC (2000) Special report on emissions secenarios, Intergovernmental Panel on Climate Change (IPCC). In: Nakicenovic N, Swart R (eds). Cambridge University Press, UK
Ishak E, Rahman A (2014) Detection of changes in flood data in Victoria, Australia over 1975–2011. Hydrol Res 46(5):763–777
Ishak E, Haddad K, Zaman M, Rahman A (2011) Scaling property of regional floods in New South Wales Australia. Nat Hazards 58:1155–1167
Ishak E, Rahman A, Westra S, Sharma A, Kuczera G (2013) Evaluating the non-stationarity of Australian annual maximum floods. J Hydrol 494:134–145
Kwarteng AY, Dorvlob AS, Kumar GTV (2009) Analysis of a 27-year rainfall data (1977–2003) in the Sultanate of Oman. Int J Climatol 29:605–617
Landsea CW, Bengtsson L, Knutson TR (2010) Impact of duration thresholds on Atlantic tropical cyclone counts. J Clim 23:2508–2519
Laz OU, Rahman A, Yilmaz A, Haddad K (2014) Trends in sub hourly, sub daily and daily extreme rainfall events in eastern Australia. J Water Clim Change 5(4):667–675
Leahy P, Kiely G, Scanlon TM (2004) Managed grasslands: a greenhouse gas sink or source? Geophys Res Lett. doi:10.1029/2004GL021161
Lelieveld J et al (2012) Climate change and impacts in the Eastern Mediterranean and the Middle East. Clim Change 114:667–687
Madsen H, Arnbjerg-Nielsen K, Mikkelsen PS (2009) Update of regional intensity-duration-frequency curves in Denmark: tendency towards increased storm intensities. Atmos Res 92:343–349
Mamoon AA, Jeorgensen NE, Rahman A, Qasem H (2013) Estimation of design rainfall in arid region: a case study for Qatar using L moments. In: 35th IAHR World Congress, Chengdu, China, pp 1–9, 8–13 Sept 2013
Mamoon AA, Jeorgensen NE, Rahman A, Qasem H (2014a) An exploratory study on the impact of climate change on design rainfalls in the State of Qatar. In: ICESSE Sydney 2014: XII international conference on environmental systems science and engineering, Sydney, Australia, vols 8, 12, Part VI, pp 727–734, 15–16 Dec 2014
Mamoon AA, Jeorgensen NE, Rahman A, Qasem H (2014b) Derivation of new design rainfall in Qatar using *L*-moments based index frequency approach. Int J Sustain Built Environ 3:111–118
Meehl G et al (2007) Global climate projections, in climate change 2007: the physical science basis. In: Solomon S et al (eds) Contribution of working group i to the fourth assessment report of the Intergovernmental Panel on Climate Change. Cambridge University Press, Cambridge, pp 747–845
Nasrallah HA, Balling RC Jr (1993) Analysis of recent climatic changes in the Arabian Gulf region. Environ Conserv 20(3):223–226
Rahman A, Bates BC, Mein RG, Weinmann PE (1999) Regional flood frequency analysis for ungauged basins in south-eastern Australia. Aust J Water Resour 3(2):199–207
Steward EJ (1989) Area reduction factors for design storm construction: joint use of rain gauge and radar data. Institute for Hydrology, Wallingford
Tryhorn L, DeGaetano A (2011) A comparison of techniques for downscaling extreme precipitation over the Northeastern United States. Int J Climatol 31(13):1975–1989
Wang D, Hagen SC, Alizad K (2013) Climate change impact and uncertainty analysis of extreme rainfall events in the Apalachicola River basin, Florida. J Hydrol 480:125–135
Yilmaz AG, Perera BJC (2014) Extreme rainfall non-stationarity investigation and intensity-frequency-duration relationship. J Hydrol Eng 19:1160–1172
Zhang X et al (2005) Trends in Middle East climate extreme indices from 1950 to 2003. J Geophys Res 110:D22104. doi:10.1029/2005JD006181